Biosensors and Bioelectronics 231 (2023) 115273

Contents lists available at ScienceDirect

Biosensors and Bioelectronics

journal homepage: www.elsevier.com/locate/bios

Nondestructive separation/enrichment and rolling circle amplification-powered sensitive SERS enumeration of circulating tumor cells *via* aptamer recognition

Jinxiang Li [a,1], Chen Dong [a,1], Hongyu Gan [a], Xinyue Gu [a], Jingjing Zhang [a], Yunfeng Zhu [a], Jingrong Xiong [a], Chunyuan Song [a,b,*], Lianhui Wang [a,**]

[a] State Key Laboratory for Organic Electronics and Information Displays, Jiangsu Key Laboratory for Biosensors, Institute of Advanced Materials (IAM), Jiangsu National Synergetic Innovation Center for Advanced Materials (SICAM), Nanjing University of Posts & Telecommunications, Nanjing, 210023, China
[b] State Key Laboratory of Applied Optics, Changchun Institute of Optics, Fine Mechanics and Physics, Chinese Academy of Sciences, Changchun, 130033, China

ARTICLE INFO

Keywords:
Circulating tumor cells
Aptamer
Surface-enhanced Raman scattering
Nondestructive release
Enumeration

ABSTRACT

Nondestructive separation/enrichment and reliable detection of extremely rare circulating tumor cells (CTCs) in peripheral blood are of considerable importance in tumor precision diagnosis and treatment, yet this remains a big challenge. Herein, a novel strategy for nondestructive separation/enrichment and ultra-sensitive surface-enhanced Raman scattering (SERS)-based enumeration of CTCs is proposed *via* aptamer recognition and rolling circle amplification (RCA). In this work the magnetic beads modified with "Aptamer (Apt)-Primer" (AP) probes were utilized to specifically capture CTCs, and then after magnetic separation/enrichment, the RCA-powered SERS counting and benzonase nuclease cleavage-assisted nondestructive release of CTCs were realized, respectively. The AP was assembled by hybridizing the EpCAM-specific aptamer with a primer, and the optimal AP contains 4 mismatched bases. The RCA enhanced SERS signal nearly 4.5-fold, and the SERS strategy has good specificity, uniformity and reproducibility. The proposed SERS detection possesses a good linear relationship with the concentration of MCF-7 cells spiked in PBS with the limit of detection (LOD) of 2 cells/mL, which shows good potential practicality for detecting CTCs in blood with recoveries ranging from 100.56% to 116.78%. Besides, the released CTCs remained good cellular activity with the normal proliferation after re-culture for 48 h and normal growth for at least three generations. The proposed strategy of nondestructive separation/enrichment and SERS-based sensitive enumeration is promising for reliable analysis of EpCAM-positive CTCs in blood, which is expected to provide a powerful tool for analysis of extremely rare circulating tumor cells in complex peripheral blood for liquid biopsy.

1. Introduction

Circulating tumor cells (CTCs) are the malignant cells that fall off solid tumors and come into the blood circulation system, and monitoring the extremely rare CTCs in peripheral blood is significant for diagnosing early tumors, predicting the invasion potential, and evaluating therapeutic efficacy and cancer prognostics (Alix-Panabières and Pantel, 2014; Chaffer and Weinberg, 2011; Plaks et al., 2013; Steeg, 2006; Yoon et al., 2014). In addition, the CTCs with good activity after the separation from complex whole blood facilitates the deep research at the molecular level to reveal the pathogenic mechanisms of cancer and explore the personalized treatment of tumors (Li et al., 2019). Therefore, the reliable separation and detection of CTCs is of great clinical importance. However, nondestructive separation and ultra-sensitive enumeration of CTCs from billions of leukocytes in peripheral blood has been a great challenge due to their extremely low abundance in complex blood (Allard et al. 2004; van de Stolpe et al., 2011; Wang et al., 2013; Xiang et al., 2023).

* Corresponding author. State Key Laboratory for Organic Electronics and Information Displays, Jiangsu Key Laboratory for Biosensors, Institute of Advanced Materials (IAM), Jiangsu National Synergetic Innovation Center for Advanced Materials (SICAM), Nanjing University of Posts & Telecommunications, Nanjing, 210023, China.
** Corresponding author.
E-mail addresses: iamcysong@njupt.edu.cn (C. Song), iamlhwang@njupt.edu.cn (L. Wang).
[1] These authors contributed equally to this work.

https://doi.org/10.1016/j.bios.2023.115273
Received 28 November 2022; Received in revised form 17 March 2023; Accepted 27 March 2023
Available online 28 March 2023

Over the past decade, many techniques have been implemented to separate CTCs from blood, such as size/density-based enrichment (Wu et al., 2018; Zhang et al., 2018), adhesion preference-based isolation (Chen et al., 2013; Yin et al., 2022; Zhang et al., 2012), and affinity-based capture (Cui et al., 2022; Li et al., 2022). Among them, the immunomagnetic beads-based separation/enrichment methods represented by the CellSearch system were widely used (Nagrath et al., 2007; Poudineh et al., 2017; Strati et al., 2021; Xiong et al., 2016). However, the cells captured *via* the immunological recognitions are difficult to be released, especially nondestructively released (Chen et al., 2019; Xiong et al., 2016). Besides, the accurate enumeration of extremely rare CTCs requires ultra-sensitive biosensor (Leung et al., 2019; Li et al., 2019). Although many detection technologies of CTCs (e.g., fluorescence (Chen et al., 2021), colorimetric assay (Xia et al., 2021), electrochemistry (Wang et al., 2019), mass spectrometry (Zhang et al., 2021) and differential pulse voltammetry (Khoshroo et al., 2022) have been developed rapidly in recent years, the reliable detection of CTC with extremely low abundance puts forward higher requirements for the more sensitive biosensors (Qin et al., 2020).

Nucleic acid aptamers are oligonucleotides, which are unique due to their secondary and tertiary structure with excellent affinity and specificity to particular proteins (Feng et al., 2011; Tan et al., 2013; Wu et al., 2014), and can act as identification elements for specific recognitions of CTCs (Ren et al., 2022; Shen et al., 2013; Song et al., 2019; Zhang et al., 2019b). In contrast to immune recognition, aptamers have unique advantages over traditional recognition element antibodies, such as synthetic and editable properties, high stability, small size, cost-effective, low immunogenicity (Miao and Tang, 2019; Yin et al., 2020). Moreover, the bio-recognition of CTCs based on the aptamers can make it possible to implement nondestructive release of cells through DNA strand displacement reaction or enzymatic digestion (Sun et al., 2016), and it can also combine the nucleic acid-based signal amplification strategy to significantly improve the sensitivity of the detection (Lu et al., 2022). Besides, the surface-enhanced Raman scattering (SERS) is well-known as a fingerprint spectrum with ultra-sensitivity for non-invasive detection (Zhang et al., 2019a), and the rolling circle amplification (RCA) is a powerful isothermal strategy for signal amplification (Sun et al., 2020).

In consideration of the advantages of aptamer recognition, SERS detection and RCA-based signal amplification, which is expected to simultaneously achieve CTC separation, enrichment, ultra-sensitive detection and non-destructive release, herein, we developed a novel strategy for nondestructive separation/enrichment and ultra-sensitive SERS enumeration of CTCs. Briefly, we designed special aptamer probes (APs) and modified them on magnetic beads (MBs) to efficiently capture and magnetically separate/enrich CTCs. Besides, a RCA-powered SERS counting and a benzonase nuclease cleavage-assisted release of CTCs were proposed for sensitive detection and nondestructive release of CTCs, respectively. The structure of double-strand "Aptamer (Apt) -Primer" (AP) probe was optimize, and then SA-the MBs@AP probes and the feasibility of RCA reaction and SERS assay were characterized. After the construction of the optimal detection condition and signal amplification of RCA, the performance on CTCs detection and nondestructive separation/enrichment of CTCs were studied. Furthermore, the potential practicality of the proposed strategy was investigated, which is expected to achieve reliable analysis of EpCAM-positive CTCs in peripheral blood and provide a powerful tool for analysis of extremely rare CTCs for liquid biopsy.

2. Experimental section

2.1. Preparation of AP-functionalized magnetic beads (MBs)

First, 15 μL of 10 mg/mL treptavidin-modified magnetic beads (SA-MBs) was magnetically washed by washing buffer (5 mM Tris-HCl, 0.5 mM EDTA, and 1 M NaCl, pH 7.4) for three times. Then, the double-stranded DNAs (dsDNAs) APs were prepared by incubating 1 μM Apt with 1 μM Primer, followed by an annealing treatment, i.e., heating the mixture at 95 °C for 5 min and then naturally cooled to room temperature. Then, 40 μL of 1 μM AP was added to 3 μL SA-MBs and incubated for 60 min at 37 °C under slight shaking. After magnetic separation and washing, the AP-functionalized MBs (SA-MBs@AP) were obtained and stored at 4 °C for further use.

2.2. Magnetic separation and enrichment of CTCs

The MCF-7 cells suspended in 180 μL PBS at different concentrations (5, 10, 50, 100, 200, 500 and 1000 cells/mL) were incubated with 20 μL SA-MBs@AP for 60 min at 37 °C under slight shaking respectively, so that to allow the SA-MBs@AP specifically absorb on the cells *via* the specific binding between the single-stranded DNAs (ssDNAs) Apt and the EpCAM proteins on cell membrane. The MCF-7 cells were then separated and enriched by an outside magnetic field, accompanied by three times PBS washing. The MCF-7 cells were then incubated with 10 μL of 1 μM ssDNAs CT for 3 h to form double-stranded DNAs (dsDNAs) PC in solution by the hybridization of Primer and CT. Then, the supernatant including PCs was extracted by magnetic separation for further RCA reaction, and the separated MBs-captured cells were dispersed in 20 μL PBS.

2.3. RCA reaction

First, 2 μL T4 ligase and 1.3 μL of 10 × T4 ligase buffer were added to the extracted supernatant and reacted at 16 °C for 16 h to make the 5′-end phosphorylated CT form a closed loop. After that, 2 μL phi29 polymerase, 2 μL of 10 × phi29 polymerase buffer, 2 μL dNTPs and 0.7 μL PBS were added into the above mixture and reacted at 30 °C for 2 h to conduct the RCA reactions, followed by heating at 65 °C for 20 min to inactivate the enzyme. The final RCA product was used for SERS detection.

2.4. SERS-based cell enumeration

The RCA products were incubated with silver nanorods (Ag NRs) array substrates for 3 h. After three times water washing, the Ag NRs substrates were incubated with 20 μL of 1 μM MCH for 10 min to block the nonspecific adsorption of RCA products on the substrates. After that, 20 μL of 1 μM Probes was incubated with the Ag NRs substrate for 3 h, and after three times water washing SERS tests on substrate were performed. For each sample, three parallel tests were conducted.

As a reference, the SERS-based cell enumeration without RCA reaction was also conducted. Briefly, 180 μL of 1000 cells/mL MCF-7 cells in PBS were incubated with 20 μL SA-MBs@AP for 60 min at 37 °C under slight shaking. After magnetic separation and PBS washing, the MCF-7 cells were then incubated with 10 μL of 1 μM CT for 3 h to form PCs. After magnetic separation, the liquid supernatant containing PCs was incubated with Ag NRs array substrate for 3 h. Then, the substrate was blocked by 20 μL of 1 μM MCH for 10 min. After that, 20 μL of 1 μM Probes was incubated with Ag NRs array for 3 h, and after three times water washing SERS tests on substrate were performed. For each sample, three parallel tests were conducted.

2.5. Cell release

The MBs-captured cells were released from the SA-MBs@AP by enzymatic digestions, i.e., 2.5 μL benzonase nuclease was added and incubated with the MBs-captured cells at 37 °C for 20 min to cleave the DNA strands and allow the release of cells. The SA-MBs were then collected by magnetic separation, and the released cells in the solution were centrifugally (750 rpm for 3 min) purified and re-dispersed in fresh DMEM for further culture.

2.6. Human blood pretreatment

The peripheral blood samples were collected in vacutainer tubes containing the anticoagulant EDTA, which were stored at 4 °C and processed within 72 h. The human blood was pretreated to remove plasma and the red blood cells. Briefly, 1 mL Histopaque-1119 reagent and 1 mL Histopaque-1077 reagent were added in 2 mL whole blood. After a centrifugation at 700 g for 30 min, the up-layer of transparent plasma, the mononuclear cell layer and the red blood cell layer were observed in sequence. The plasma was removed and the mononuclear cell layer was transferred to a new 15 mL centrifuge tube and centrifuged twice at 200 g for 10 min. Finally, the separated cells were suspended in 1 mL PBS for further use. The study was approved by the Medical Ethical Committee of the Jiangsu Provincial People's Hospital (Nanjing, China) (No. 2021-SR-110).

3. Results and discussion

3.1. Working mechanism of the CTC separation, SERS enumeration and nondestructive release

Fig. 1 shows a schematic illustration of the nondestructive separation/enrichment and RCA-powered SERS-based sensitive enumeration of CTCs *via* aptamer recognition. Firstly, the biotin-labeled aptamer (Apt) hybridizes with SH-labeled Primer by annealing treatment to form the dsDNAs Apt-Primer (AP) with a lock-like structure (i.e., including several mismatched bases), then the APs are modified on the surface of streptavidin-modified magnetic beads (SA-MBs) *via* the specific combination of biotin and streptavidin. The AP-modified magnetic beads (SA-MBs@AP) are incubated with CTCs (e.g., human breast cancer cell MCF-7 as an analysis model) to allow the SA-MBs@AP link to cells *via* the specific recognition and combination of the specific Apts and the corresponding EpCAM proteins on cells. The combination of Apts and EpCAM proteins makes part of the base-pairs of AP unwound. Then, the SA-MBs@AP-captured cells in the solution are separated by exerting external magnetic field, i.e., the separation and enrichment of CTCs from the complex solution are achieved. After that, the SA-MBs@AP-captured cells are incubated with CT which can hybridize with the Primer on the SA-MBs and make the hybrid (i.e., PC) fall off the SA-MBs. Therefore, after magnetic separation, the SA-MBs@AP-captured cells can be separated from the PCs in the supernatant. Furthermore, on the one hand, the SA-MBs@AP-captured cells are incubated with benzonase nuclease which can digest the nucleic acids on the cells to nondestructively release the cells from the SA-MBs. The SA-MBs can be collected by magnetic separation for reuse, and the cells can be cleaned and collected by centrifugal separation for further analysis. On the other hand, the PCs in the supernatant are mixed with T4 to make the 5′-end phosphorylated CT form a closed loop, and then the RCA reactions were conducted by adding Phi29 polymerase and dNTPs. Therefore, the ssDNAs generated by RCA (RCA products) include tandem repeats. The RCA products are modified onto the Ag NRs SERS-active substrate *via* S–Ag covalent bonds, and after blocking of the Ag NRs substrate with MCH, the substrate is incubated with ROX-labeled Probes to allow the hybridization between ROX-labeled Probes and the tandem repeats. So that, strong SERS signals can be detected since a considerable number of ROX-labeled Probes are captured on the Ag NRs substrate, and the cells in the sample can be quantified according to the detected SERS signals. In conclusion, the proposed strategy can not only realize the efficient, specific and nondestructive separation/enrichment of CTCs from the complex solution, but also can achieve high-sensitive SERS detection *via* the enrichment of CTCs and the RCA-powered signal amplification.

3.2. Optimization of the AP

The AP with a lock-like structure can specifically and efficiently bind to the cells *via* the combination between Apts and EpCAM proteins on cells, which makes partial bases of the Primer unwound from the base-pairs of AP while the remained complementary base-pairs facilitated the enrichment of Primers and CTCs from the complex sample solution by magnetic separation. Then, the exposed/unwound bases of Primer can be served as the toehold for hybridization with CT to form PC (Primer + CT) as the initial element of the RCA reaction. Fig. 2a shows a schematic illustration of the AP structure in which some bases (i.e., mismatched bases) of Primer is not complementary to Apt. For

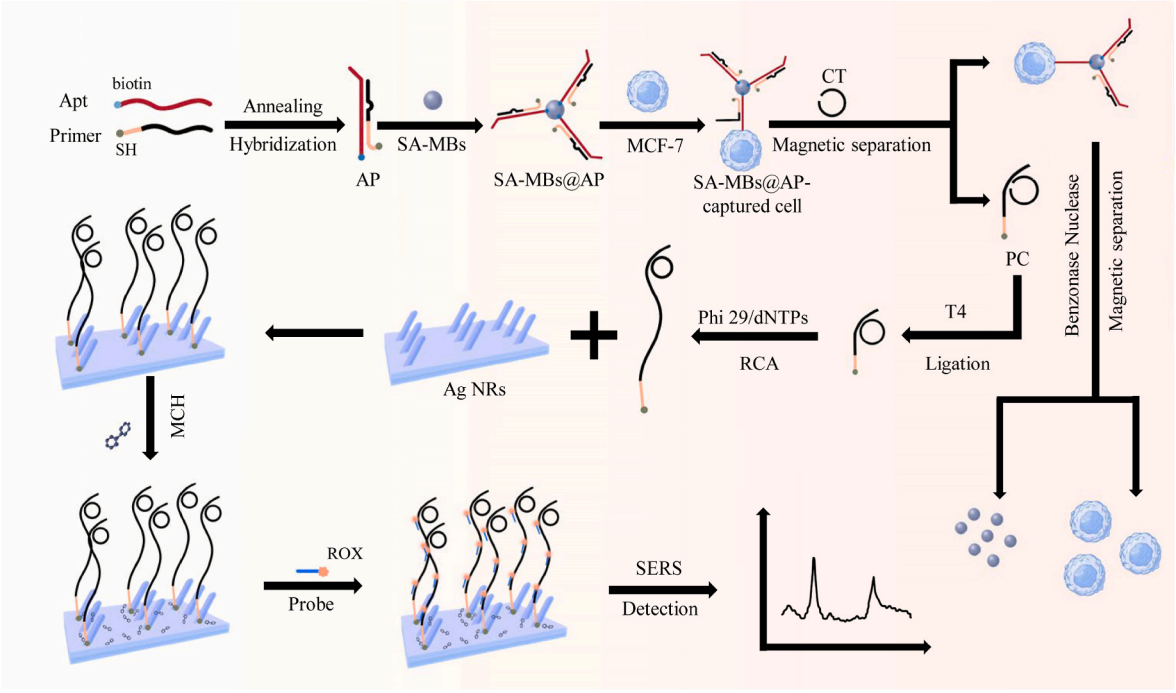

Fig. 1. Schematic illustration of the construction of SA-MBs@AP and the working principle of nondestructive separation/enrichment and rolling circle amplification-powered SERS-based sensitive enumeration of circulating tumor cells *via* aptamer recognition.

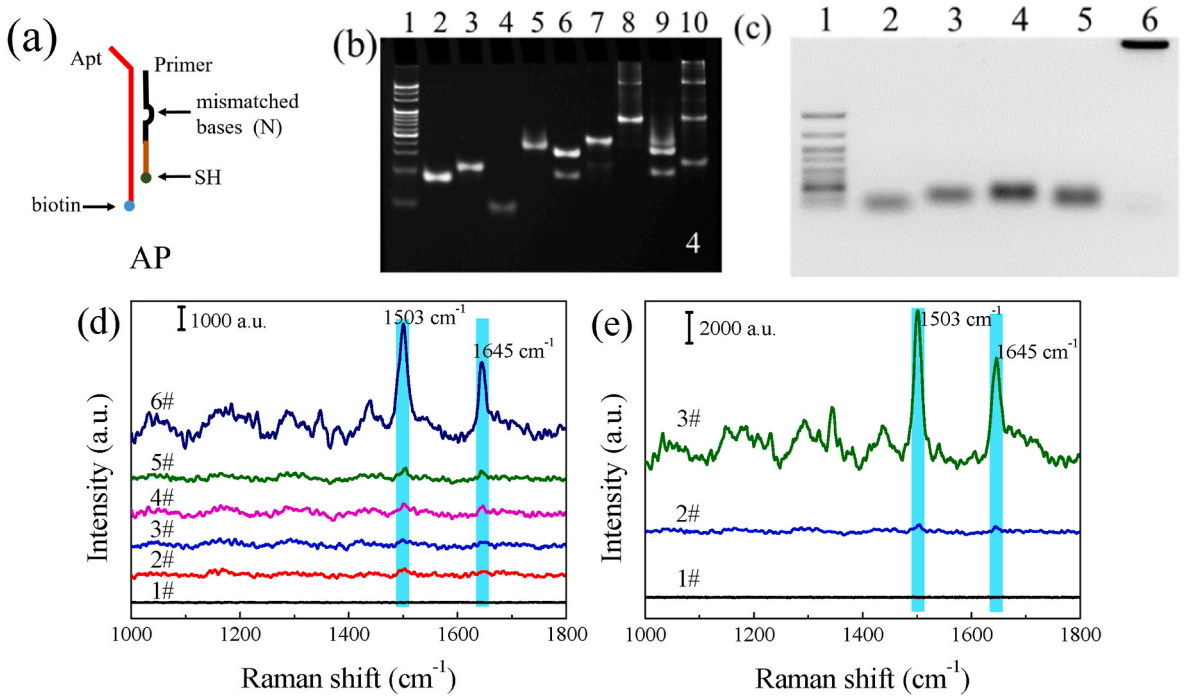

Fig. 2. Characterizations of the feasibility of CTCs separation/enrichment and SERS detection. (a) Schematic illustrations of a AP with mismatched bases. (b) Electrophoretic pattern for characterizing the sensing mechanism by using the AP with the mismatched bases of 4. Lane 1: Marker, lane 2: Apt-4, lane 3: Apt-4-open, lane 4: Primer, lane 5: CT, lane 6: Apt-4 + Primer, lane 7: Apt-4-open + Primer, lane 8: Primer + CT, lane 9: Apt-4 + Primer + CT, lane 10: Apt-4-open + Primer + CT. (c) Agarose gel electrophoresis for characterizing the RCA reaction. Lane 1: 5000 bp Marker, lane 2: Primer, lane 3: CT, lane 4: Primer + CT, lane 5: Primer + CT + T4, lane 6: Primer + CT + T4 + phi29 DNA polymerase + dNTPs. (d) SERS spectra for characterizing the RCA-powdered sensing strategy. 1#: Ag NRs, 2#: Primer-Ag NRs + Probe, 3#: CT-Ag NRs + Probe, 4#: (Primer + CT)-Ag NRs + Probe, 5#: (Primer + CT) + T4-Ag NRs + Probe, 6#: RCA-Ag NRs + Probe. (e) Characterizations of the feasibility of SERS detection of MCF-7 cells. 1#: Ag NRs, 2#: Ag NRs + RCA + MCH + Probe +0 cell/mL, 3#: Ag NRs + RCA + MCH + Probe +1000 cells/mL.

investigation of the optimal AP, the AP structure containing different number (N) of mismatched bases, i.e., N = 0, 4, 6 and 8, were designed, and the corresponding Apts were named Apt-N, i.e., Apt-0, Apt-4, Apt-6, and Apt-8 (Table S2, Section S1, Supporting Information (SI)).

As shown in Fig. S1a (Section S2, SI), the scenario of AP without mismatched bases (i.e., N = 0) is not considered to form PC duplex as expected. Furthermore, the electrophoresis characterizations of different mismatched bases in AP (i.e., N = 4, 6 and 8, respectively) are shown in Fig. 2b (N = 4), Fig. S1b (N = 6, Section S2, SI) and Fig. S1c (N = 8, Section S2, SI). Similar to the analysis of N = 0, according to the results of lane 6 in these electrophoresis patterns, all the three Apts can hybridize with Primer to form double-stranded APs. The lanes 7 indicates that the corresponding Apt-N-opens can hybridize with the Primer stably. In addition, when Apt-4 (6 or 8) hybridized with Primer, the strips in lane 9 could not be observed in the same position as the strips in lane 8, which indicates that the CT could not competitively hybridize with the Primer in the AP. However, when Apt-4 (6 or 8)-open replaced Apt-4 (6 or 8), the strips in lane 10 are similar to the strips in lane 8, and the slight strip with the fastest migration corresponding to Apt-4 (6 or 8)-open occurred, indicating that the PC (Primer + CT) as the initial reactant of RCA reaction can be generated when CT was incubated with the duplex of Apt-4 (6 or 8)-open and Primer. Besides, only the strips belonging to CT (lane 5) and AP (lane 6) appeared in lane 9 of N = 4, while the hybrid of Primer and CT (lane 8) also appeared in lane 9 of N = 6 and N = 8. These results indicate that N = 6 and 8 have certain false positives, which would make the final detection results biased with poor detection sensitivity. Therefore, the number of 4 of mismatched bases is the optimal selection.

3.3. Feasibility of RCA reaction and SERS assay

Fig. 2c shows the agarose gel electrophoresis for characterizing the RCA reaction. The lanes 1 to 3 show the strips of Marker (5000 bp), Primer, and CT, respectively. The slowly moved strip in lane 4 relative to the one in lane 3 indicates the hybridization of Primer and CT, which was also confirmed by the strips shown in the lanes 5, 6 and 8 in Fig. 2b. The bright strip at the top of lane 6 which contained the mixture of Primer, CT, T4, phi29 DNA polymerase and dNTPs confirms that the RCA reactions occurred successfully and the RCA products with big structure were formed.

The TEM image, zeta potential and cytotoxicity of the SA-MBs@AP probes were characterized and shown in Fig. S2 and Table S3 (Section S3, SI), and the results indicate that the SA-MBs@AP probes with good biocompatibility were successfully prepared. According to the TEM image shown in Figs. S2a and b, there is no significant differences in size or morphology between the SA-MBs and SA-MBs@AP, and the APs modified on SA-MBs were difficult to be observed from the TEM image. Considering the effective cell separation and the possible concentration-related self-aggregation of MBs (Freitas et al., 2020; Shen et al., 2021; Wen et al., 2014), the 150 μg/mL SA-MBs@AP probes was selected for cell separation and enrichment in the standard sensing strategy. Fig. 2d shows the SERS spectra collected from the Ag NRs substrates before (1#) and after the incubation with Probes and different mixtures: 2# Primer; 3# CT, 4# Primer and CT; 5# Primer, CT and T4; 6# RCA product. After washing, only the RCA products generated the characteristic SERS peaks of ROX molecules at 1503 and 1645 cm^{-1}, which confirms that the RCA products can capture the Probes onto the Ag NRs successfully. Therefore, the successful implementation of the RCA reactions and the effective RCA-based SERS sensing are verified.

Fig. 2e shows the feasibility of RCA-based SERS detection of MCF-7

cells. The bare Ag NRs (1#, black) shows very low background, and the sample in the absence of MCF-7 cells (0 cells/mL) was selected as the control (2#, blue line). The typical SERS signals of ROX at 1503 and 1645 cm^{-1} were identified when tested the sample containing 1000 cells/mL (3#, green), which can be significantly distinguished from the control. Therefore, the proposed sensing strategy for separation/enrichment and RCA-powered SERS-based sensitive enumeration of circulating tumor cells is feasible.

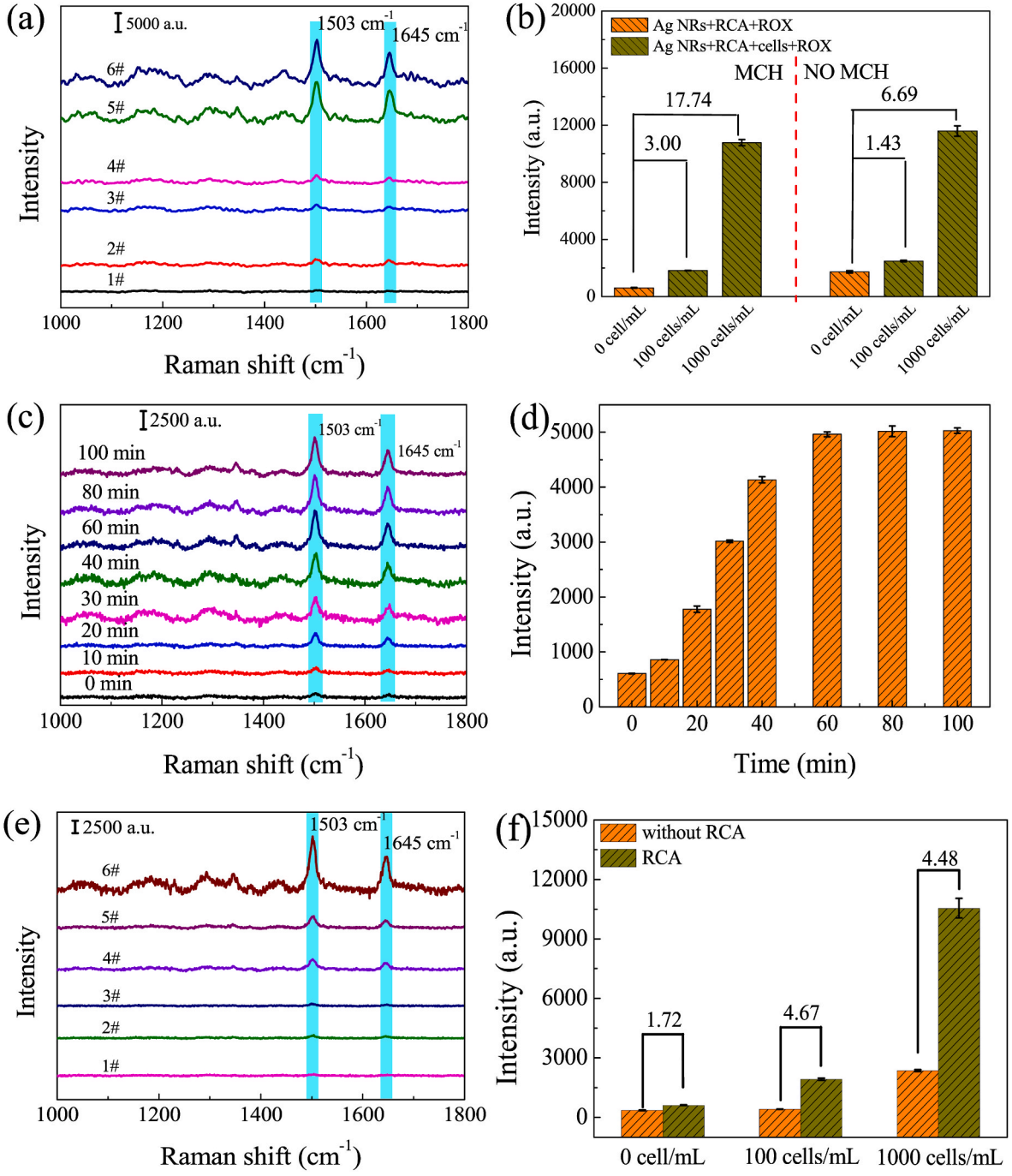

Fig. 3. Optimization of MCH blocking, incubation time and exploration of RCA amplification. (a) SERS spectra collected from the detections of 0, 100 and 1000 cells/mL in the absence or presence of MCH blocking. 1#: Ag NRs + (RCA-0 cell/mL) + MCH + Probe, 2#: Ag NRs + (RCA-0 cell/mL) + Probe, 3#: Ag NRs + (RCA-100 cells/mL) + MCH + Probe, 4#: Ag NRs + (RCA-100 cells/mL) + Probe, 5#: Ag NRs + (RCA-1000 cells/mL) + MCH + Probe, 6#: Ag NRs + (RCA-1000 cells/mL) + Probe. (b) Plot of the signal intensities of ROX at 1503 cm^{-1} corresponding to the spectra shown in (a), and the signal-to-noise ratios (S/N). (c) SERS spectra collected from the detections of 500 cells/mL conducted by incubating SA-MBs@AP probes with cells with different incubation times, i.e., 0, 10, 20, 30, 40, 60, 80 and 100 min, respectively. (d) Plot of the signal intensities of ROX at 1503 cm^{-1} corresponding to the spectra shown in (c). (e) SERS spectra collected from the detections of 0, 100 and 1000 cells/mL with or without RCA amplification. 1#: Ag NRs + (m-Primer-0 cell/mL) + MCH + Probe, 2#: Ag NRs + (RCA-0 cell/mL) + MCH + Probe, 3#: Ag NRs + (m-Primer-100 cells/mL) + MCH + Probe, 4#: Ag NRs + (RCA-100 cells/mL) + MCH + Probe, 5#: Ag NRs + (m-Primer-1000 cells/mL) + MCH + Probe, 6#: Ag NRs + (RCA-1000 cells/mL) + MCH + Probe. (f) Plot of the signal intensities of ROX at 1503 cm^{-1} corresponding to the spectra shown in (e). All error bars represent standard deviations from three measurements (n = 3).

3.4. Characterization of the binding of APs to MCF-7 cells

Fig. S3 (Section S4, SI) shows the fluorescence images of FAM-APs treated cells. Almost no fluorescence of FAM was collected from the blank MCF-7 cells. The green fluorescence from FAM-APs-treated EpCAM-positive cells (i.e., MCF-7 and DU145 cells) is much higher than the signal from the HeLa cells (i.e., EpCAM-negative cells), which indicates that the APs can specifically target the EpCAM proteins on cell membranes, and the Kd of APs on MCF-7 cells is 27 ± 4 nM (Fig. S4, Section S4, SI). The results demonstrate that the APs exhibit good binding affinity toward the EpCAM-positive MCF-7 cells, and endows the high capability of SA-MBs@AP for specifically capturing CTCs.

3.5. Optimization of detection conditions

Optimization of MCH blocking of Ag NRs. The optimal MCH blocking may effectively improve the specificity of the sensing. Fig. 3a shows the SERS spectra of the tests of 0 (blank), 100, and 1000 cells/mL with or without MCH blocking, respectively. Due to the non-specific adsorption of RCA produces and Probe, the SERS signal intensity of

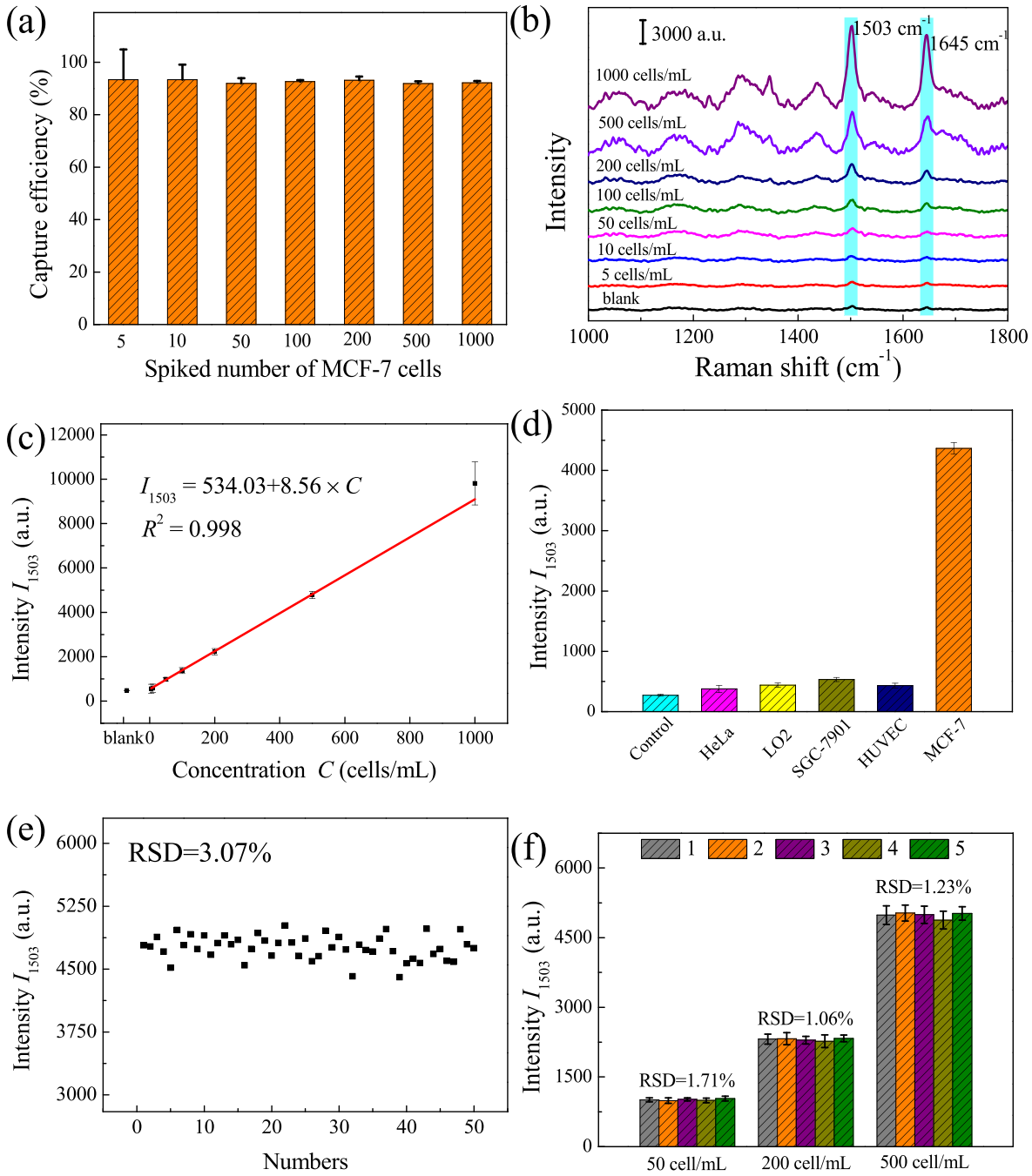

Fig. 4. Enrichment and detection of CTCs in PBS. (a) Capture efficiency of SA-MBs@AP probes for capturing different numbers (5, 10, 50, 100, 200, 500 and 1000 cells) of MCF-7 cells spiked in PBS. Error bars represent standard deviations from three measurements (n = 3). (b) SERS spectra of the detections of MCF-7 cells in PBS with different concentrations, i.e., blank (without cells), 5, 10, 50, 100, 200, 500 and 1000 cells/mL. (c) Plot of the concentration-dependent SERS intensity I_{1503} in (b). Error bars represent the standard deviations from ten measurements (n = 10). (d) Plot of the signal intensities of ROX at 1503 cm^{-1} corresponding to the spectra shown in Fig. S7. (e) Plot of SERS signal intensitied at 1503 cm^{-1} corresponding to the SERS spectra shown in Fig. S8(a). (f) Plot of SERS signal intensities at 1503 cm^{-1} corresponding to the SERS spectra shown in Fig. S8(b)–(d).

ROX molecules recorded from the Ag NRs without MCH blocking was higher than that of the MCH blocking group no matter the tested cells concentrations. The characteristic SERS signals of ROX at 1503 cm^{-1} plotted in Fig. 3b indicate that the improved signal-to-noise ratios (S/N) of 3.00 for 100 cells/mL and 17.74 for 1000 cells/mL were obtained. These results conclude that the MCH blocking is essential to obtain specific detection and is favorable to achieve low detection limit.

Optimization of incubation time. Fig. 3c shows the SERS spectra detected under different incubation times (0–100 min) for incubation of SA-MBs@AP probes with MCF-7 cells. Along with the increasing incubation time, stronger SERS signal was outputted, and after incubation for 60 min, the SERS signal reached a saturation (Fig. 3d), which means the optimal incubation time can be selected as 60 min.

Optimization of RCA time. Fig. S5a (Section S5, SI) shows the SERS assay spectra of 100 cells/mL MCF-7 cells with different RCA reaction times (0–180 min). The SERS signal at 1503 cm^{-1} increases gradually with the increasing RCA time. After incubation for 120 min, the SERS signal reached a saturation (Fig. S5b, Section S5, SI), and the optimal RCA reaction time was selected as 120 min.

3.6. Signal amplification of RCA

Fig. S3 shows the schematic diagram of the assay without RCA (Section S4, SI). The MCF-7 cells in PBS with concentrations of 0 and 1000 cells/mL were SERS tested with or without RCA, respectively. The SERS spectra of assays were shown in Fig. 3e, and as the SERS intensities plotted in Fig. 3f, with the RCA amplification, the background signal (0 cells/mL) enhanced 1.72 times, and nearly 4.5 times signal amplification was obtained when tested 1000 cells/mL MCF-7 cells. Specifically, the SERS assay of 100 cells/mL MCF-7 cells without RCA amplification was not clearly different from the blank control, that is, the detection without RCA is not conducive to obtaining sensitive assay with lower detection limit, which indicates that the RCA signal amplification-based SERS detection of cells is a superior choice for sensitive CTCs enumeration.

3.7. Performance on CTCs detection

Capture Efficiency. Under the optimal conditions, the performance of SA-MBs@AP on the capture of CTC was investigated by incubating the SA-MBs@AP with different numbers of MCF-7 spiked in PBS, i.e., 5, 10, 50, 100, 200, 500 and 1000 cells, respectively. Fig. 4a shows that the capture efficiencies are about 93%, calculated according to the following equation: capture efficiency = (1-n/N) × 100%, where n is the number of uncaptured cells and N is the total number of cells spiked in the sample observed and counted by optical microscope after capture by SA-MBs@AP. All the results were obtained from three independent experiments. It should be noted that despite the differences in the concentrations of CTCs, the capture efficiency is relatively stable, which facilitates the capture of cells at low concentrations.

Calibration curve and limit of detection (LOD). Under the above-mentioned optimal conditions, the concentration-related SERS assays of MCF-7 cells (blank, 5, 10, 50, 100, 200, 500 and 1000 cells/mL) in PBS were conducted and the SERS spectra are shown in Fig. 4b. The SERS signal intensity of ROX gradually increases with the increasing MCF-7 cells concentration, and the SERS signal can still be distinguished from the blank even the cell concentration is low to 5 cells/mL. The SERS signal intensity at 1503 cm^{-1} (I_{1503}) plotted in Fig. 4c follows a good linear relationship with the concentration (C) of MCF-7 cells, i.e., $I_{1503} = 534.03 + 8.56 \times C$ ($R^2 = 0.998$), and the LOD was calculated to be 2 cells/mL (S/N = 3), which is superior to most previously reported aptamer-based CTC detections (Table S4, Section S7, SI).

Specificity. Fig. S7 (Section S8, SI) presents the SERS spectra obtained by testing specific MCF-7 cells (EpCAM-positive cells), and unspecific cells (EpCAM-negative cells, including human umbilical vein endothelial cells (HUVEC), human gastric cancer cells (SGC-7901), normal human hepatocytes (LO2) and human cervical cancer cells (HeLa)), as well as PBS without any cells (blank). The SERS signal of MCF-7 cells detection is significantly higher than those of the unspecific or blank detections, which indicates a good specificity of the proposed sensing strategy for MCF-7 cells detection (Fig. 4d).

Uniformity and reproducibility. Fig. S8a (Section S9, SI) shows the SERS spectra of the assay of 500 cells/mL MCF-7 cells recorded from 50 random points (Section S6, SI), and the relative standard deviation (RSD) of the SERS intensities at 1503 cm^{-1} plotted in Fig. 4e is within 3.07%, which indicates that the proposed sensing strategy has good uniformity. For characterizing the reproducibility, the MCF-7 cells with the concentrations of 50, 200 and 500 cells/mL were tested respectively. For each cell concentration, 5 parallel tests were conducted and the averaged SERS spectra randomly recorded at 8 points were shown in Figs. S8b–d (Section S9, SI), corresponding to 50, 200 and 500 cells/mL, respectively (Section S6, SI). The SERS intensities at 1503 cm^{-1} were plotted in Fig. 4f, which shows very small variations of the three detections with the RSDs less than 2%, indicating that the proposed CTCs sensing strategy has good reproducibility.

Potential practicality. For investigating the potential practicality of the SERS strategy for detecting CTCs in blood, the erythrocytes (white blood cells, WBCs) in blood were extracted by centrifugation and used as the background cells of CTCs assay. Briefly, the WBCs in the whole blood of healthy human were extracted and then MCF-7 cells were spiked in the WBCs (5×10^6 cells/mL) to prepare test samples with different concentrations of MCF-7 cells (i.e., blank, 5, 10, 50, 100, 200, 500 and 1000 cells/mL). The samples were tested by the SERS sensing strategy and the spectra are shown in Fig. 5a. The SERS intensity at 1503 cm^{-1} (I_{1503}) plotted in Fig. 5b follows a good linear relationship with the concentration of MCF-7 cells (C) spiked in WBCs, i.e., $I_{1503} = 487.22 + 9.25 \times C$ ($R^2 = 0.989$). The LOD of MCF-7 cells in WBCs was calculated to be 3 cells/mL (S/N = 3). The recoveries of 50, 250 and 500 cells/mL MCF-7 cells in WBCs were studied and 5 parallel tests were conducted for each concentration. Fig. 5c shows the averaged SERS spectra of the assays. According to the SERS intensities at 1503 cm^{-1} and the calibration curve, the found cell concentrations are listed in Fig. 5d, which shows good recoveries ranging from 100.56% to 116.78% with the RSD less than 13.95%. The high recovery rate indicates that the high capture efficiency can guarantee the accuracy of the detection (Fig. S9, Section S10, SI). Despite the small differences between the capture efficiency and recovery rate, but considering the experimental systematic error and the recovery rate calculated from the calibration curve rather than the real number of cells in the sample, the result still indicates a relatively good consistency between the isolated and measured CTCs. Therefore, the proposed SERS-based RCA-powered detection of CTCs is promising for reliably counting CTCs in blood.

3.8. Nondestructive separation and enrichment of CTCs

Nondestructive separation and enrichment of CTCs are particularly favorable for the downstream cell analysis. Benzonase nuclease, which is a highly useful endonuclease for the removal of nucleic acids from recombinant proteins and protein fragments by completely digesting nucleic acids to 5′-monophosphate terminated oligonucleotides 2–5 bases in length (Yin et al., 2020), was used to effectively cut the DNAs connection between the MBs and cell membrane proteins for nondestructive release of cells. The captured CTCs were released by the cleavage of benzonase nuclease, and the activity of released cells were than cultured. Fig. 6a–f shows the normal proliferation of the cells after re-culture for 0–48 h, and the cells can grow normally after three generations (Fig. 6g and h), which indicates that the cells still had good cellular activity. The MCF-7 cells released from different concentrations of SA-MBs@AP probes (i.e., 100, 125, 150, 175 and 200 μg/mL) after benzonase nuclease treatment were used as experimental groups, while the same number of MCF-7 cells which digested from culture flask by trypsin were served as control. The cells were cultured in 96-well plates,

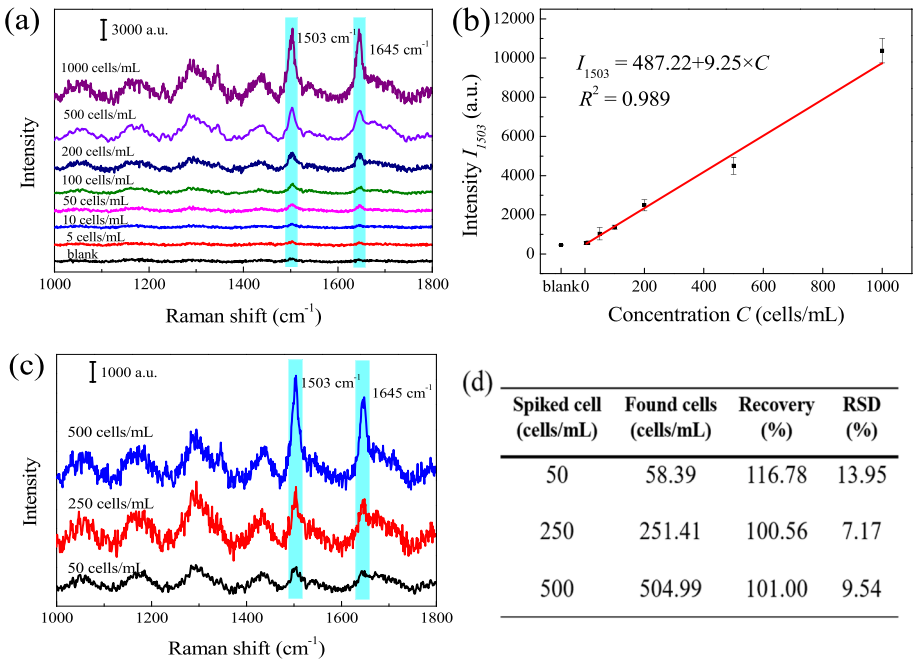

(d)

Spiked cell (cells/mL)	Found cells (cells/mL)	Recovery (%)	RSD (%)
50	58.39	116.78	13.95
250	251.41	100.56	7.17
500	504.99	101.00	9.54

Fig. 5. SERS detections of CTCs in WBCs with different MCF-7 cell concentrations, i.e., blank (without cells), 5, 10, 50, 100, 200, 500 and 1000 cells/mL. (a) SERS spectra of the detections of MCF-7 in WBCs. (b) Plot of the concentration-dependent SERS intensity I_{1503} in (a). Error bars represent the standard deviations (n = 10). (c) Characterization of recovery for detecting MCF-7 cells in WBCs with the concentration of 50 cells/mL, 250 cells/mL and 500 cells/mL. (d) Recovery of MCF-7 cells spiked in WBCs.

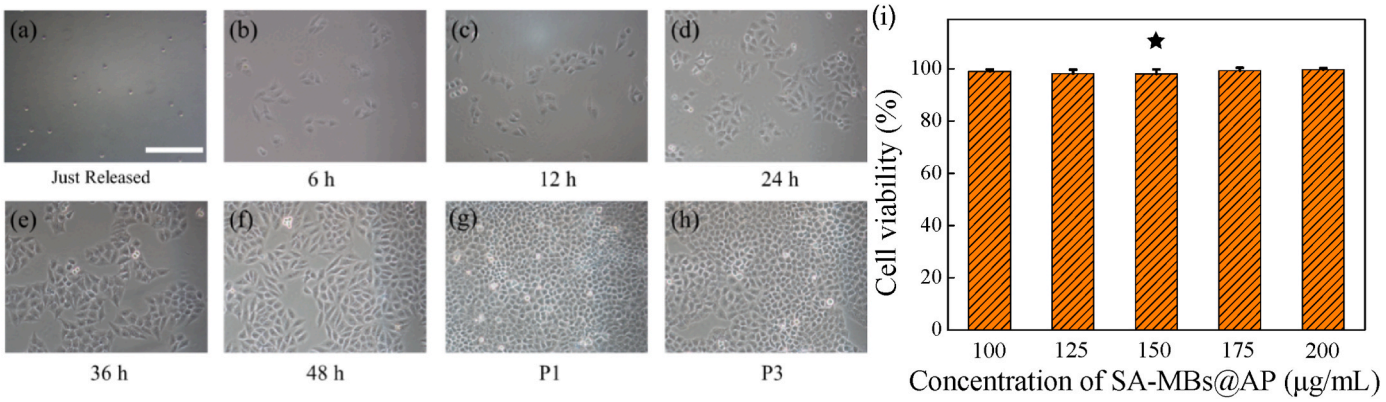

Fig. 6. Activity of the post-released CTCs. (a)–(h) Microscopic images of the post-released cells after re-culture for 0–48 h, and the cell proliferation and growth after 1 passage (P1) (g) and 3 passages (P3) (h). Scale bar 100 μm. (i) Cell viability of MCF-7 cells released from SA-MBs@AP probes with different concentrations, i.e., 100, 125, 150, 175 and 200 μg/mL. Error bars represent standard deviations from three measurements (n = 3).

and the MTT assays were conducted by using the MTT assay kit. Fig. 6i shows the viabilities of cells released from different concentrations of SA-MBs@AP probes (i.e., 100, 125, 150, 175 and 200 μg/mL) after benzonase nuclease treatment, and the MTT results indicate that the released cells have good biological activity.

To characterize the nondestructive release of CTCs by benzonase nuclease, the fluorescence images of MCF-7 cells before and after the treatment of benzonase nuclease were scanned. As shown in Fig. S10 (Section S11, SI), the MCF-7 cells treated by FAM-labeled APs show distinct green fluorescence. After the treatment of benzonase nuclease, the green fluorescence on the cell membrane disappeared since the FAM-labeled aptamers in APs were degraded. Furthermore, the treated MCF-7 cells after benzonase nuclease treatment can capture FAM-labeled APs again and show bright fluorescence of FAM, which indicates that the benzonase nuclease can effectively remove the aptamers on the cells without causing obvious side effects to the EpCAM membrane proteins and their functions.

3.9. Reuse of SA-MBs

The MBs-captured cells were incubated with benzonase nuclease to nondestructively release the cells from the SA-MBs. Herein, the MCF-7 cells with the concentrations of 100 and 500 cells/mL were SERS detected, respectively. The magnetically separated cells were released by benzonase nuclease treatment. Then the cells were collected by centrifugation and the SA-MBs were collected by magnetic separation. The SA-MBs were used for the next detection of cells. Fig. S11a (Section S12, SI) shows the SERS spectra of the assays of 100 and 500 cells/mL by using the fresh SA-MBs (1#) or the SA-MBs after one (2#) and two (3#) reuse batches. The signal intensities of ROX at 1503 cm^{-1} corresponding to the spectra shown in Fig. S11a (Section S12, SI) after each detection were summarized in Fig. S11b (Section S12, SI). It can be seen that there was no significant decrease in SERS signal intensities, which indicates that three repeats did not affect the performance of SA-MBs on cell detection.

4. Conclusions

In summary, we propose a novel strategy for nondestructive separation/enrichment and SERS-based ultra-sensitive enumeration of circulating tumor cells, in which the magnetic beads modified with special APs (SA-MBs@AP) were utilized to capture the CTCs *via* the combination of the specific Apts and the EpCAM proteins on cells, and then the magnetically separated/enriched CTCs were SERS counted *via* RCA and nondestructive released by the cleavage of benzonase nuclease. The optimal AP contains 4 mismatched bases, which can minimize the false-positives and -negative detections. Taking the MCF-7 cells as the analysis model of CTCs, the preferred incubation time between SA-MBs@AP and cells is 60 min, and the MCH blocking is essential to obtain specific detection and is favorable to achieve low detection limit. The RCA is a preferred signal amplification for sensitive SERS-based CTCs enumeration, and nearly 4.5 times SERS signal enhancement was obtained. The SERS strategy possesses a good linear relationship with the concentration of MCF-7 cells spiked in PBS with the LOD of 2 cells/mL. Besides, the proposed strategy has the advantages of good specificity, uniformity, and reproducibility. The investigation of potential practicality for detecting CTCs in blood shows good recoveries ranging from 100.56% to 116.78%, which indicates that the proposed SERS-based RCA-powered detection of CTCs is promising for reliably counting CTCs in blood. Furthermore, the nondestructive separation/enrichment of CTCs was effectively achieved by digesting the nucleic acids with benzonase nuclease. Therefore, the proposed strategy is expected to provide a powerful tool for high-sensitively counting and nondestructively separating/enriching EpCAM-positive CTCs.

CRediT authorship contribution statement

Jinxiang Li: Methodology, Investigation, Data curation, Writing – original draft. **Chen Dong:** Methodology, Formal analysis, Writing – original draft. **Hongyu Gan:** Data curation. **Xinyue Gu:** Formal analysis. **Jingjing Zhang:** Validation. **Yunfeng Zhu:** Formal analysis. **Jingrong Xiong:** Investigation. **Chunyuan Song:** Conceptualization, Funding acquisition, Writing – review & editing. **Lianhui Wang:** Project administration, Supervision.

Declaration of competing interest

The authors declare that they have no known competing financial interests or personal relationships that could have appeared to influence the work reported in this paper.

Data availability

Data will be made available on request.

Acknowledgements

This work was financially supported by the National Key Research and Development Program of China (2017YFA0205300), National Natural Science Foundation of China (61871236, 62235008, 62288102, and 61971207), State Key Laboratory of Applied Optics (SKLAO2022001A08), and Qinglan Project of Jiangsu Province of China.

Appendix A. Supplementary data

Supplementary data to this article can be found online at https://doi.org/10.1016/j.bios.2023.115273.

References

Alix-Panabières, C., Pantel, K., 2014. Challenges in circulating tumour cell research. Nat. Rev. Cancer 14 (9), 623–631.
Allard, W.J., Matera, J., Miller, M.C., Repollet, M., Connelly, M.C., Rao, C., Tibbe, A.G.J., Uhr, J.W., Terstappen, L.W.M.M., 2004. Tumor cells circulate in the peripheral blood of all major carcinomas but not in healthy subjects or patients with nonmalignant diseases. Clin. Cancer Res. 10 (20), 6897–6904.
Chaffer, C.L., Weinberg, R.A., 2011. A perspective on cancer cell metastasis. Science 331 (6024), 1559–1564.
Chen, J., Yu, L., Li, Y., Cuellar-Camacho, J.L., Chai, Y., Li, D., Li, Y., Liu, H., Ou, L., Li, W., Haag, R., 2019. Biospecific monolayer coating for multivalent capture of circulating tumor cells with high sensitivity. Adv. Funct. Mater. 29 (33), 1808961.
Chen, P., Wang, Y., He, Y., Huang, K., Wang, X., Zhou, R., Liu, T., Qu, R., Zhou, J., Peng, W., Li, M., Bai, Y., Chen, J., Huang, J., Geng, J., Xie, Y., Hu, W., Ying, B., 2021. Homogeneous visual and fluorescence detection of circulating tumor cells in clinical samples via selective recognition reaction and enzyme-free amplification. ACS Nano 15 (7), 11634–11643.
Chen, W., Weng, S., Zhang, F., Allen, S., Li, X., Bao, L., Lam, R.H.W., Macoska, J.A., Merajver, S.D., Fu, J., 2013. Nanoroughened surfaces for efficient capture of circulating tumor cells without using capture antibodies. ACS Nano 7 (1), 566–575.
Cui, M., Chen, X., Luo, X., Zhou, Z., Chen, Z., Zhou, Z., Zhou, X., Zou, H., Xu, T., Wang, S., Yang, M., 2022. Dually stimulative single-chain polymeric nano lock with dynamic ligands for sensitive detection of circulating tumor cells. Biosens. Bioelectron. 217 (1), 114692.
Feng, K., Qiu, L.-P., Yang, Y., Wu, Z.-S., Shen, G.-L., Yu, R.-Q., 2011. Label-free optical bifunctional oligonucleotide probe for homogeneous amplification detection of disease markers. Biosens. Bioelectron. 29 (1), 66–75.
Freitas, M., Nouws, H.P.A., Keating, E., Delerue-Matos, C., 2020. High-performance electrochemical immunomagnetic assay for breast cancer analysis. Sensors Actuat. B-Chem. 308, 127667.
Khoshroo, A., Fattahi, A., Hosseinzadeh, L., 2022. Development of paper-based aptasensor for circulating tumor cells detection in the breast cancer. J. Electroanal. Chem. 910, 116182.
Leung, C.-H., Wu, K.-J., Li, G., Wu, C., Ko, C.-N., Ma, D.-L., 2019. Application of label-free techniques in microfluidic for biomolecules detection and circulating tumor cells analysis. Trends Anal. Chem. 117, 78–83.
Li, C., Li, R., Wu, X., Zuo, Y., Xiong, G., Huang, M., Sun, Y., Liao, R., Xiao, Y., Hu, L., Gao, C., Yu, Y., 2022. Capture of heterogeneous circulating tumor cells in colorectal cancer patients on an immunomagnetic and anti-nonspecific adsorption platform. Anal. Chem. 94 (44), 15240–15249.
Li, W., Wang, H., Zhao, Z., Gao, H., Liu, C., Zhu, L., Wang, C., Yang, Y., 2019. Emerging nanotechnologies for liquid biopsy: the detection of circulating tumor cells and extracellular vesicles. Adv. Mater. 31 (45), 1805344.
Lu, B., Deng, Y., Peng, Y., Huang, Y., Ma, J., Li, G., 2022. Fabrication of a polyvalent aptamer network on an electrode surface for capture and analysis of circulating tumor cells. Anal. Chem. 94 (37), 12822–12827.
Miao, P., Tang, Y., 2019. Gold nanoparticles-based multipedal DNA walker for ratiometric detection of circulating tumor cell. Anal. Chem. 91 (23), 15187–15192.
Nagrath, S., Sequist, L.V., Maheswaran, S., Bell, D.W., Irimia, D., Ulkus, L., Smith, M.R., Kwak, E.L., Digumarthy, S., Muzikansky, A., Ryan, P., Balis, U.J., Tompkins, R.G., Haber, D.A., Toner, M., 2007. Isolation of rare circulating tumour cells in cancer patients by microchip technology. Nature 450 (7173), 1235–1239.
Plaks, V., Koopman, C.D., Werb, Z., 2013. Circulating tumor cells. Science 341 (6151), 1186–1188.
Poudineh, M., Aldridge, P.M., Ahmed, S., Green, B.J., Kermanshah, L., Nguyen, V., Tu, C., Mohamadi, R.M., Nam, R.K., Hansen, A., Sridhar, S.S., Finelli, A., Fleshner, N. E., Joshua, A.M., Sargent, E.H., Kelley, S.O., 2017. Tracking the dynamics of circulating tumour cell phenotypes using nanoparticle-mediated magnetic ranking. Nat. Nanotechnol. 12 (3), 274–281.
Qin, W., Chen, L., Wang, Z., Li, Q., Fan, C., Wu, M., Zhang, Y., 2020. Bioinspired DNA nanointerface with anisotropic aptamers for accurate capture of circulating tumor cells. Adv. Sci. 7 (19), 2000647.
Ren, X.-H., Han, D., He, X.-Y., Guo, T., Chen, X.-S., Pang, X., Cheng, S.-X., 2022. Multi-targeting nano-systems targeting heterogeneous cancer cells for therapeutics and biomarker detection. Adv. Healthc. Mater., 2202155
Shen, C., Zhong, L., Xiong, L., Liu, C., Yu, L., Chu, X., Luo, X., Zhao, M., Liu, B., 2021. A novel sandwich-like cytosensor based on aptamers-modified magnetic beads and carbon dots/cobalt oxyhydroxide nanosheets for circulating tumor cells detection. Sensors Actuat. B-Chem. 331, 129399.
Shen, Q., Xu, L., Zhao, L., Wu, D., Fan, Y., Zhou, Y., Ouyang, W.H., Xu, X., Zhang, Z., Song, M., Lee, T., Garcia, M.A., Xiong, B., Hou, S., Tseng, H.R., Fang, X., 2013. Specific capture and release of circulating tumor cells using aptamer-modified nanosubstrates. Adv. Mater. 25 (16), 2368–2373.
Song, Y., Shi, Y., Huang, M., Wang, W., Wang, Y., Cheng, J., Lei, Z., Zhu, Z., Yang, C., 2019. Bioinspired engineering of a multivalent aptamer-functionalized nanointerface to enhance the capture and release of circulating tumor cells. Angew. Chem. Int. Ed. 131 (8), 2258–2262.
Steeg, P.S., 2006. Tumor metastasis: mechanistic insights and clinical challenges. Nat. Med. 12 (8), 895–904.
Strati, A., Zavridou, M., Kallergi, G., Politaki, E., Kuske, A., Gorges, T.M., Riethdorf, S., Joosse, S.A., Koch, C., Bohnen, A.-L., Mueller, V., Koutsodontis, G., Kontopodis, E., Poulakaki, N., Psyrri, A., Mavroudis, D., Georgoulias, V., Pantel, K., Lianidou, E.S., 2021. A comprehensive molecular analysis of in vivo isolated EpCAM-positive circulating tumor cells in breast cancer. Clin. Chem. 67 (10), 1395–1405.

Sun, N., Liu, M., Wang, J., Wang, Z., Li, X., Jiang, B., Pei, R., 2016. Chitosan nanofibers for specific capture and nondestructive release of CTCs assisted by pCBMA brushes. Small 12 (36), 5090–5097.
Sun, S., Yang, S., Hu, X., Zheng, C., Song, H., Wang, L., Shen, Z., Wu, Z.-S., 2020. Combination of immunomagnetic separation with aptamer-mediated double rolling circle amplification for highly sensitive circulating tumor cell detection. ACS Sens. 5 (12), 3870–3878.
Tan, W., Donovan, M.J., Jiang, J., 2013. Aptamers from cell-based selection for bioanalytical applications. Chem. Rev. 113 (4), 2842–2862.
van de Stolpe, A., Pantel, K., Sleijfer, S., Terstappen, L.W., den Toonder, J.M.J., 2011. Circulating tumor cell isolation and diagnostics: toward routine clinical use. Cancer Res. 71 (18), 5955–5960.
Wang, L., Asghar, W., Demirci, U., Wan, Y., 2013. Nanostructured substrates for isolation of circulating tumor cells. Nano Today 8 (4), 374–387.
Wang, S.-S., Zhao, X.-P., Liu, F.-F., Younis, M.R., Xia, X.-H., Wang, C., 2019. Direct plasmon-enhanced electrochemistry for enabling ultrasensitive and label-free detection of circulating tumor cells in blood. Anal. Chem. 91 (7), 4413–4420.
Wen, C.-Y., Wu, L.-L., Zhang, Z.-L., Liu, Y.-L., Wei, S.-Z., Hu, J., Tang, M., Sun, E.-Z., Gong, Y.-P., Yu, J., Pang, D.-W., 2014. Quick-response magnetic nanospheres for rapid, efficient capture and sensitive detection of circulating tumor cells. ACS Nano 8 (1), 941–949.
Wu, L., Ren, J., Qu, X., 2014. Target-responsive DNA-capped nanocontainer used for fabricating universal detector and performing logic operations. Nucleic Acids Res. 42 (21) e160-e160.
Wu, M., Huang, P.H., Zhang, R., Mao, Z., Chen, C., Kemeny, G., Li, P., Lee, A.V., Gyanchandani, R., Armstrong, A.J., Dao, M., Suresh, S., Huang, T.J., 2018. Circulating tumor cell phenotyping via high-throughput acoustic separation. Small 14 (32), e1801131.
Xia, N., Wu, D., Yu, H., Sun, W., Yi, X., Liu, L., 2021. Magnetic bead-based electrochemical and colorimetric assays of circulating tumor cells with boronic acid derivatives as the recognition elements and signal probes. Talanta 221, 121640.
Xiang, Y., Hu, C., Wu, G., Xu, S., Li, Y., 2023. Nanomaterial-based microfluidic systems for cancer biomarker detection: recent applications and future perspectives. Trends Anal. Chem. 158, 116835.
Xiong, K., Wei, W., Jin, Y., Wang, S., Zhao, D., Wang, S., Gao, X., Qiao, C., Yue, H., Ma, G., Xie, H.-Y., 2016. Biomimetic immuno-magnetosomes for high-performance enrichment of circulating tumor cells. Adv. Mater. 28 (36), 7929–7935.
Yin, X., Chen, B., He, M., Hu, B., 2020. A multifunctional platform for the capture, release, and enumeration of circulating tumor cells based on aptamer binding, nicking endonuclease-assisted amplification, and inductively coupled plasma mass spectrometry detection. Anal. Chem. 92 (15), 10308–10315.
Yin, Z., Shi, R., Xia, X., Li, L., Yang, Y., Li, S., Xu, J., Xu, Y., Cai, X., Wang, S., Liu, Z., Peng, T., Peng, Y., Wang, H., Ye, M., Liu, Y., Chen, Z., Tan, W., 2022. An implantable magnetic vascular scaffold for circulating tumor cell removal in vivo. Adv. Mater., 2207870
Yoon, H.J., Kozminsky, M., Nagrath, S., 2014. Emerging role of nanomaterials in circulating tumor cell isolation and analysis. ACS Nano 8 (3), 1995–2017.
Zhang, J., Yang, Y., Jiang, X., Dong, C., Song, C., Han, C., Wang, L., 2019a. Ultrasensitive SERS detection of nucleic acids via simultaneous amplification of target-triggered enzyme-free recycling and multiple-reporter. Biosens. Bioelectron. 141, 111402.
Zhang, N., Deng, Y., Tai, Q., Cheng, B., Zhao, L., Shen, Q., He, R., Hong, L., Liu, W., Guo, S., Liu, K., Tseng, H.R., Xiong, B., Zhao, X.Z., 2012. Electrospun TiO_2 nanofiber-based cell capture assay for detecting circulating tumor cells from colorectal and gastric cancer patients. Adv. Mater. 24 (20), 2756–2760.
Zhang, X., Liu, C., Pei, Y., Song, W., Zhang, S., 2019b. Preparation of a novel Raman probe and its application in the detection of circulating tumor cells and exosomes. ACS Appl. Mater. Interfaces 11 (32), 28671–28680.
Zhang, X., Wei, X., Men, X., Wu, C.-X., Bai, J.-J., Li, W.-T., Yang, T., Chen, M.-L., Wang, J.-H., 2021. Dual-multivalent-aptamer-conjugated nanoprobes for superefficient discerning of single circulating tumor cells in a microfluidic chip with inductively coupled plasma mass spectrometry detection. ACS Appl. Mater. Interfaces 13 (36), 43668–43675.
Zhang, Y., Wang, Z., Wu, L., Zong, S., Yun, B., Cui, Y., 2018. Combining multiplex SERS nanovectors and multivariate analysis for in situ profiling of circulating tumor cell phenotype using a microfluidic chip. Small 14 (20), e1704433.